

Article

Not peer-reviewed version

---

# Optical Wireless Communication with Intelligent Reflecting Surfaces

---

[Chengwei Fang](#)<sup>\*</sup>, [Shuo Li](#), Yinong Wang, [Ke Wang](#)

Posted Date: 5 August 2024

doi: 10.20944/preprints202408.0223.v1

Keywords: Optical wireless communication; intelligent reflecting surfaces; mirror array; metasurface



Preprints.org is a free multidiscipline platform providing preprint service that is dedicated to making early versions of research outputs permanently available and citable. Preprints posted at Preprints.org appear in Web of Science, Crossref, Google Scholar, Scilit, Europe PMC.

Copyright: This is an open access article distributed under the Creative Commons Attribution License which permits unrestricted use, distribution, and reproduction in any medium, provided the original work is properly cited.

Disclaimer/Publisher's Note: The statements, opinions, and data contained in all publications are solely those of the individual author(s) and contributor(s) and not of MDPI and/or the editor(s). MDPI and/or the editor(s) disclaim responsibility for any injury to people or property resulting from any ideas, methods, instructions, or products referred to in the content.

Article

# Optical Wireless Communication with Intelligent Reflecting Surfaces

Chengwei Fang <sup>1,\*</sup>, Shuo Li <sup>1</sup>, Yinong Wang <sup>2</sup> and Ke Wang <sup>1</sup>

<sup>1</sup> School of Engineering, Royal Melbourne Institute of Technology (RMIT) University, Melbourne, VIC 3000, Australia (e-mail: s3643273@student.rmit.edu.au; shuo.li2@rmit.edu.au; ke.wang@rmit.edu.au).

<sup>2</sup> School of Architecture and Urban Design, Royal Melbourne Institute of Technology (RMIT) University, Melbourne, VIC 3000, Australia (e-mail: s3576616@student.rmit.edu.au).

\* Correspondence: s3643273@student.rmit.edu.au

Academic Editor: Firstname Lastname

**Abstract:** Optical Wireless Communication (OWC) technology has gained significant attention in recent years due to its potential to provide high data rate wireless connections through the large license-free bandwidth available. A key challenge in OWC systems, similar to high-frequency Radio Frequency (RF) systems, is the presence of dead zones caused by obstacles like buildings, trees, and moving individuals, which can degrade signal quality or disrupt data transmission. Traditionally, relays have been used to mitigate these issues. Intelligent Reflecting Surfaces (IRS) have recently emerged as a promising solution, enhancing system performance and flexibility by providing reconfigurable communication channels. This paper presents an overview of the application of IRS in OWC systems. Specifically, we categorize IRS into two main types: mirror array-based IRS and metasurface-based IRS. Furthermore, we delve into modeling approaches of mirror array-based IRS in OWC and analyze recent advances in IRS control, which are classified into system power or gain optimization oriented, system link reliability optimization oriented, system data rate optimization oriented, and system security optimization oriented approaches. Finally, we discuss the key challenges and potential future directions for integrating IRS with OWC systems, providing insights for further research in this promising field.

**Keywords:** Optical wireless communication; intelligent reflecting surfaces; mirror array; metasurface.

## 1. Introduction

With the rapid development of science and technology, the demand for high-speed wireless communications has surged, particularly driven by bandwidth-intensive applications such as high-definition video-on-demand, virtual reality, and augmented reality [1]. However, the congested microwave spectrum has caused conventional RF wireless communication systems to struggle to meet these bandwidth and speed demands [2,3]. To overcome these limitations, Beyond Fifth-Generation (B5G) has attracted significant attention for its potential to provide high-speed wireless connections through large, license-free bandwidths. B5G is envisioned to rely on a variety of wireless technologies, including Millimeter-wave (mmWave), Terahertz (THz) communications, and OWC [4], as summarized in Tab. 1.

Millimeter-wave communication has been explored for short to moderate-distance data transmission, typically ranging from tens to hundreds of meters. However, mmWave suffers from high path loss and sensitivity to blockages, which limit its effective transmission distance and require advanced techniques like beamforming and Multiple-Input-Multiple-Output (MIMO) to maintain reliable connections [5]. Similarly, THz communication offers even larger bandwidths and higher data rates, potentially reaching tens to hundreds of Gigabits per Second (Gbps) [6]. However, THz waves face even higher attenuation and are highly sensitive to atmospheric conditions, limiting their transmission distance to a few meters to several hundreds of meters under ideal conditions [7].

In comparison, OWC has been proposed and widely studied for its potential to achieve much higher data rates, reaching up to Terabits per Second (Tbps), thanks to the vast license-free bandwidth available in the optical spectrum. Additionally, OWC is more cost-effective compared to THz communications, utilizing low-cost transceivers such as Light-Emitting Diodes (LEDs) and Photodiodes

(PDs) [8–10]. Free Space Optics (FSO), a type of OWC, extends these benefits over longer distances, making it suitable for applications like space-based communications. Despite these advantages, OWC, like mmWave and THz communications, faces significant challenges related to the vulnerability of signals to obstructions, which can cause considerable signal loss and degradation, or even complete communication interruption [11–14]. The short wavelength of optical signals leads to higher penetration loss and increased vulnerability to shadowing and blockages, which can create coverage gaps and negatively impact the system's performance and Quality of Service (QoS) [4].

**Table 1.** Comparisons of B5G wireless communication technologies.

	mmWave systems	THz systems	OWC system	FSO system
<b>Distance</b>	Long (Several kilometers in ideal conditions, tens to hundreds of meters in urban environments)	Short (a few meters to several hundreds of meters in ideal conditions)	Limited (Tens to hundreds of meters indoors)	Several kilometers (can be much longer in space-based systems (Lunar-to-Earth or deep space))
<b>Carrier Frequency</b>	Low (30 GHz to 300 GHz)	Moderate (0.1 THz to 10 THz)	High (Hundreds of THz)	High (Hundreds of THz)
<b>Bandwidth</b>	Several GHz	Tens to hundreds of GHz	Broad (in the order of THz)	Broad (in the order of THz)
<b>Data Rate</b>	Tens of Gbps	Tens to hundreds of Gbps	Tbps	Tbps

To mitigate these challenges, innovative solutions are required to ensure robust and reliable wireless systems. Techniques such as adaptive optics [15], diversity schemes [16,17], and the use of IRS have been proposed to enhance signal propagation and overcome the limitations posed by obstacles [18]. Among these, IRSs are highly promising due to the unique capability to dynamically manipulate the wireless propagation channels. IRSs are planar arrays of resonant sub-wavelength elements designed to manipulate the phase of incident beams across their surface to achieve desired directionality, such as anomalous reflection, following the generalized law of reflection. However, for optical applications, conventional mirrors, which primarily reflect light without phase manipulation, do not fall into this category [19,20]. In IRS-based RF systems, IRSs belong to the broader category of metasurfaces, altering various properties of electromagnetic waves such as amplitude, phase, dispersion, momentum, and polarization [18]. In OWC systems, IRSs are typically categorized into two types: mirror array-based IRS and metasurface-based IRS. Mirror array-based IRS controls the optical signal path by adjusting the orientation of mirrors within the IRS matrix to intelligently vary the signal reflection angle and guide the signal towards the receiver, enhancing system performance [21,22]. Meta-surface-based IRS, on the other hand, uses nanotechnology and materials science to design reflective surfaces that perform beamforming, reducing interference and beam wastage, and increasing the system gain [23,24].

Compared to their application in RF systems, IRSs in OWC systems exhibit distinct differences and advantages. In RF communication systems, IRSs primarily enhance signal propagation and extend coverage by optimizing reflection phases. However, in OWC systems, IRSs must optimize both communication performance and illumination when the optical communication systems serve dual roles of lighting and communication, such as in Visible Light Communication (VLC). This optimization is not necessarily required for near-infrared systems, which are typically used solely for communication purposes. The unique characteristics of optical signals require IRS designs to consider beam shaping and the receiver's Field of View (FOV) to ensure adequate illumination and communication link quality [4]. Additionally, while IRS deployment in RF systems typically occurs between the transmitter and the receiver, IRSs in OWC systems can be placed at the transmitter, receiver, or along the transmission path, depending on functional and performance optimization needs [22,25–28]. This flexibility allows IRSs

in optical communication systems to more precisely control signal propagation, effectively overcoming the challenges posed by complex environments, such as urban areas with dense buildings, indoor settings with numerous obstacles, and outdoor environments with varying weather conditions.

In recent years, a number of surveys and summary papers on IRSs have been published, which are summarized in Tab. 2. In [29], a brief review of the recent applications and design aspects of IRS in future wireless networks is presented. The paper introduces the basic concepts and reconfigurability of IRS, discusses the joint optimization of IRS phase control with transceiver transmission control, and analyzes performance improvements in various network design problems. In [30] and [31], the principles, performance analysis, and challenges of using IRS to enhance wireless network coverage and data rates are reviewed. These papers discuss RIS hardware, control mechanisms, and channel models, presenting performance analyses using various parameters and metrics. They also address the challenges of integrating IRS into wireless networks, focusing on channel estimation and deployment comparisons for single and multi-user scenarios, and propose future research directions for IRS-assisted wireless communication systems. In [32], the up-to-date research on IRS-aided wireless communications is further comprehensively reviewed, focusing on solutions to practical design issues such as channel estimation and passive beamforming, and discussing new and emerging IRS architectures and applications. All of the above papers focus on IRS in RF systems, highlighting the significant research interest and advancements in this area.

While the IRS has predominantly been applied in traditional RF systems, recent survey papers have also reviewed THz wireless communication systems incorporating IRSs. [33] reviews the integration of IRS in THz communications for 6G networks, discussing application scenarios such as mobile communications, secure communications, Unmanned Aerial Vehicles (UAV), Mobile Edge Computing (MEC), and THz localization. It also examines enabling technologies like hardware design, channel estimation, and beam control, while highlighting challenges and open problems in IRS-empowered THz communications. [34] focuses on performance analysis and future promising applications of IRS-enabled THz communications, highlighting the role of IRSs in enhancing link reliability and data rates to support emerging intelligent applications.

Furthermore, the IRS has also been reviewed from an application-oriented perspective, such as 6G vehicular communications and UAV communications. [35] surveys current research on the application of IRS in 6G vehicular communications, both ground-based and aerial, highlighting IRS's role in enhancing signal strength, security, and positioning accuracy. Moreover, [36] surveys the integration of IRS and UAVs in communications, discussing existing literature, emerging technologies, application scenarios, and future research directions to enhance spectrum and energy efficiencies.

**Table 2.** Recent surveys and the comparison with this paper.

Reference	Year	Area of focus
<b>RF Systems</b>		
Gong et al. [29]	2020	<ul style="list-style-type: none"> <li>• IRS applications and design in future wireless networks</li> <li>• Concepts and reconfigurability</li> <li>• Joint optimization</li> <li>• Performance improvements</li> </ul>
Hassouna et al. [30], [31]	2023	<ul style="list-style-type: none"> <li>• IRS in enhancing wireless networks</li> <li>• Hardware, control, and channel models</li> <li>• Performance metrics</li> <li>• Challenges</li> </ul>
Zheng et al. [32]	2022	<ul style="list-style-type: none"> <li>• IRS-aided wireless communications</li> <li>• Design issues</li> <li>• New architectures</li> <li>• Applications</li> </ul>
<b>mmWave/THz Systems</b>		
Chen et al. [33]	2021	<ul style="list-style-type: none"> <li>• IRS in THz communications for 6G</li> <li>• Application scenarios</li> <li>• Enabling technologies</li> <li>• Challenges</li> </ul>
Raza et al. [34]	2022	<ul style="list-style-type: none"> <li>• IRS in THz communication for B5G/6G</li> <li>• Performance analysis</li> <li>• Enhancing reliability and data rates</li> </ul>
Zhu et al. [35]	2022	<ul style="list-style-type: none"> <li>• IRS in 6G vehicular communications</li> <li>• Signal strength and security</li> <li>• Positioning accuracy</li> </ul>
Mohsan et al. [36]	2022	<ul style="list-style-type: none"> <li>• IRS and UAV integration</li> <li>• Literature and technologies</li> <li>• Application scenarios</li> </ul>
<b>OWC Systems</b>		
Abumarshoud et al. [25]	2021	<ul style="list-style-type: none"> <li>• RIS-assisted LiFi systems</li> <li>• RIS architecture</li> <li>• Operational elements</li> <li>• Major challenges</li> </ul>
Sylvester et al. [4]	2023	<ul style="list-style-type: none"> <li>• RIS in OWC systems</li> <li>• Indoor applications</li> <li>• Key challenges</li> </ul>
This survey	2024	<ul style="list-style-type: none"> <li>• IRS in OWC systems</li> <li>• Mirror array models</li> <li>• Recent developments</li> <li>• Major challenges and Future Scope</li> </ul>

While IRS technology has shown potential in RF and THz systems, its application in OWC is promising yet underexplored. OWC offers vast unlicensed bandwidth and high data rates but faces challenges like physical obstructions and sensitivity to alignment. Integrating IRS can enhance OWC by improving signal propagation and link reliability. However, only a limited number of papers have reviewed the application of IRS in OWC systems. In [4], a comprehensive tutorial on using IRS in OWC systems is provided, focusing on indoor applications. It covers the basics of OWC and IRS, the differences between optical IRSs and RF-IRSs, key challenges in IRS-assisted OWC systems, and future

research directions integrating IRS with emerging technologies. In [25], a comprehensive overview of IRS-assisted LiFi systems is presented, exploring the underlying IRS architecture from a physics perspective and outlining potential operational elements supported by IRS-enabled transceivers and environments. It also highlights major challenges and promising future research directions. Although the previous survey papers have included the IRS aspect, they failed to review recent achievements in IRS techniques in OWC systems. For instance, [4] is a tutorial focusing on fundamental principles rather than recent progress. On the other hand, [25] focuses on a particular LiFi system with IRS, providing insights specific to their system rather than an overview of the entire research field. Therefore, this survey provides a comprehensive review of the recent developments of IRS applications in OWC systems, which include:

- A brief introduction and summary of the mirror array-based IRS model in OWC systems.
- A detailed review of the recent development of mirror array-based and metasurface-based IRS in OWC systems.

The rest of this survey is organized as follows: in Section 2, we introduce the general architecture and principles of mirror array-based IRS in OWC systems and summarize recent applications in UOWC systems. In Section 3, we provide a detailed review of metasurface-based IRS applied in recent UOWC progress. Finally, we conclude the survey and discuss the key challenges and potential future directions for integrating IRS with OWC systems in Section 4, offering insights for further research in this promising field.

## 2. Mirror Array-Based IRS in OWC Systems

IRS represents a cutting-edge technology in OWC systems. IRS can be broadly categorized into two main types: mirror array-based IRS and metasurface-based IRS. Both types aim to reconfigure incident signals and manipulate them in intelligent ways to improve communication performance. This section focuses on the mirror array-based IRS, and the metasurface-based type will be reviewed in the next section.

Mirror array-based IRS utilizes adjustable mirror arrays to change the propagation of optical signals in OWC systems. Each mirror element in the array can be independently adjusted in real time, allowing precise control over the spatial phase and direction of the light path. This technology enables the control of reflected signal directions so that all waves can converge at a single point (anomalous reflection) rather than reflecting in a uniform manner as with a flat reflector [4]. In the case of a curved reflector, the reflections can be directed towards different focal points depending on the curvature and design.

The control mechanism for mirror array-based IRS involves the use of ultra-fast switching components such as varactors, Positive-Intrinsic-Negative (PIN) diodes, or Micro-Electromechanical Systems (MEMS) switches, which communicate with a central controller [4]. Unlike traditional fixed metasurfaces, many modern tunable metasurfaces and IRS controllers can autonomously detect environmental changes and utilize intelligent algorithms to adapt in real-time [37–39]. In RF communication systems, IRS controllers can dynamically adjust the phase and amplitude of reflected signals to optimize performance. In OWC, adaptive techniques are employed to manage signal direction and phase, though the technology is still evolving to match the versatility found in RF systems.

This capability supports the dense deployment of IRS in wireless communication networks, enabling efficient manipulation of transmitted and reflected waves to optimize the communication channel and improve signal propagation in both RF and OWC systems. The real-time adaptability of IRS controllers helps address challenges such as obstacles, user movement, and varying environmental conditions, enhancing overall network performance.

Understanding the fundamental principles and benefits of mirror array-based IRS in OWC systems lays the groundwork for effective implementation. To fully leverage these advantages, it is crucial to develop accurate and comprehensive models of OWC systems with mirror array-based IRS. These models are essential for predicting system performance, optimizing signal propagation, and

addressing potential challenges in real-world deployments. In the following section, we review the methodologies and techniques for modeling OWC systems with mirror array-based IRS.

### 2.1. OWC System Model with Mirror Array-Based IRS

Recent research has extensively explored the application of IRS in indoor OWC [21,22,40,41] and FSO communication systems [18,42–44]. In indoor OWC systems, transmitters are typically LEDs with wide beam divergence, which allows them to cover a large communication area. Conversely, in FSO communication systems, transmitters are usually Laser Diodes (LDs), which provide higher power and more focused beams to counteract the losses associated with long-distance communication.

Given the growing demand for high-speed and reliable wireless communication in indoor environments, modeling mirror array-based IRS in indoor OWC systems becomes particularly important. These environments often face unique challenges such as multipath reflections and obstructions caused by furniture and other users. In this section, we focus on modeling mirror array-based IRS specifically for indoor OWC systems. As shown in Figure 1, the general indoor OWC system considered includes a mirror array IRS based on an LED transmitter and a user's PD receiver. The channel gain between the transmitter and receiver can be expressed by [4]:

$$G = IG_{\text{LOS}} + G_{\text{NLOS}}, \quad (1)$$

in this review, it is assumed that the variable  $I \in \{0, 1\}$  represents whether the Line-of-Sight (LOS) link is available or blocked.  $G_{\text{LOS}}$  and  $G_{\text{NLOS}}$  denote the channel gain of the LOS path and the Non-Line-of-Sight (NLOS) path, respectively.

The channel gain of the LOS path  $G_{\text{LOS}}$  can be expressed by:

$$G_{\text{LOS}} = \begin{cases} \frac{(m+1)A_{\text{PD}}}{2\pi d^2} \cos^m(\Phi) T(\xi) G(\xi) \cos(\xi), & 0 \leq \xi \leq \xi_{\text{FOV}} \\ 0, & \xi > \xi_{\text{FOV}}, \end{cases} \quad (2)$$

where  $m = -\frac{\ln 2}{\ln(\cos \Phi_{1/2})}$  is the Lambertian order with  $\Phi_{1/2}$  representing the semi-angle at half emitted optical power,  $A_{\text{PD}}$  is the capture area of the PD,  $d$  denotes Euclidean distance between the LED transmitter and the receiver,  $\Phi$  denotes the optical irradiance angle of the LED,  $\xi$  is the incident angle of the signal light to the receiver,  $T(\xi)$  represents the gain of the receiver optical filter, and  $G(\xi)$  denotes the gain of a concentrator, which is given by  $G(\xi) = \frac{f^2}{\sin^2 \xi_{\text{FOV}}}$ ,  $0 \leq \xi \leq \xi_{\text{FOV}}$ , where  $\xi_{\text{FOV}}$  is the FOV of the PD and  $f$  denotes the refraction index of optical concentrator. It is worth mentioning that  $\xi$  depends on the receiver's orientation.

The NLOS channel can be considered in two parts: (i) from the LED transmitter to the IRS, with the IRS serving as the receiver; (ii) from the IRS to the PD, with the IRS considered as the source that re-emits the optical signal [4]. Due to the accuracy requirements and the diminishing strength of higher-order reflections, only the first-order reflections are considered in the analysis of IRS in OWC systems. The mirror-array IRS is divided into  $\mathcal{K}$  squared surfaces with the  $k$ -th surface having an area  $dA_k$  [24]. Similar to previous work [4,24,45], it is assumed that the incident ray from the transmitter strikes the center of the reflective surfaces.

The channel gain of the NLOS path in Stage (i) with the  $k$ -th IRS serving as the receiver can be expressed as:

$$G_{\text{NLOS}}^{\text{Stage i}} = \rho_{\text{IRS}} \frac{(m+1)dA_k}{2\pi^2(d_k^a)^2} \cos^m(\Phi_k^a) \cos(\xi_k^a), \quad (3)$$

where  $\rho_{\text{IRS}}$  is the reflection coefficient of the IRS element,  $d_k^a$  represent the distance between the transmitter with the  $k$ -th reflective surface,  $\Phi_k^a$  is the irradiance angle from transmitter to the  $k$ -th reflective surface,  $\xi_k^a$  is the signal incidence angle to the  $k$ -th reflective surface.

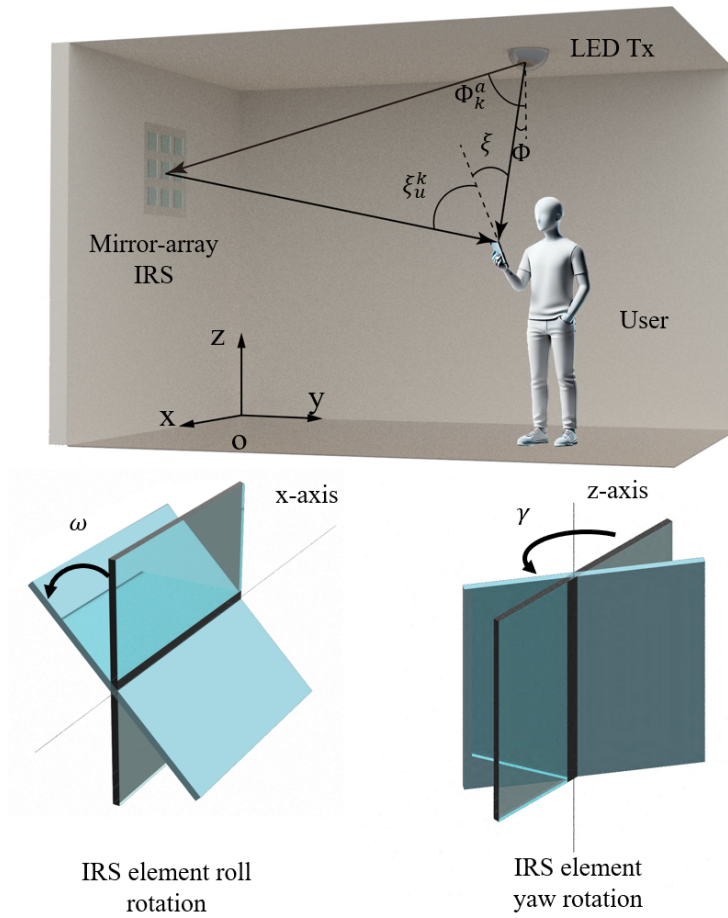


Figure 1. Mirror array IRS-based indoor OWC systems.

The channel gain of the NLOS path in Stage (ii) with the  $k$ -th IRS serving as the source can be expressed as:

$$G_{\text{NLOS}}^{\text{Stage ii}} = \begin{cases} \frac{A_{\text{PD}}}{(d_k^u)^2} \cos(\Phi_u^k) \cos(\zeta_u^k) T(\xi) G(\xi), & 0 \leq \zeta_u^k \leq \zeta_{\text{FOV}} \\ 0, & \zeta_u^k > \zeta_{\text{FOV}}, \end{cases} \quad (4)$$

where  $d_k^u$  represent the distance between the  $k$ -th reflective surface and the receiver,  $\Phi_u^k$  is the irradiance angle from the  $k$ -th reflective surface to the receiver, and  $\zeta_u^k$  is the signal incidence angle to the receiver from the  $k$ -th reflective surface. It needs to be mentioned that the cosine of the angle of irradiance (which is specified by the roll angle  $\omega$  and yaw angle  $\gamma$  of the mirror array) is [4,24]:

$$\cos(\Phi_u^k) = \frac{(x_k - x_u)}{d_k^u} \cos(\omega) + \frac{(y_k - y_u)}{d_k^u} \sin(\gamma) \cos(\omega) + \frac{(z_k - z_u)}{d_k^u} \sin(\omega), \quad (5)$$

where  $(x_k, y_k, z_k)$  represent the coordinates of the  $k$ -th IRS, and  $(x_u, y_u, z_u)$  represent the coordinates of the receivers.

Combine Eq. 3 and Eq. 4, the channel gain of the NLOS path with mirror array-based IRS system from the  $k$ -th surface can be expressed as [4,24]:

$$G_{\text{NLOS}}^{\text{IRS}_k}(\gamma, \omega) = G_{\text{NLOS}}^{\text{Stage i}} \times G_{\text{NLOS}}^{\text{Stage ii}} = \begin{cases} \rho_{\text{IRS}} \frac{(m+1)A_{\text{PD}}}{2\pi^2(d_k^t)^2(d_k^u)^2} dA_k \cos^m(\Phi_k^a) \cos(\zeta_k^a) \\ \quad \times \cos(\Phi_u^k) \cos(\zeta_u^k) T(\xi) G(\xi), & 0 \leq \zeta_u^k \leq \zeta_{\text{FOV}} \\ 0, & \zeta_u^k > \zeta_{\text{FOV}}, \end{cases} \quad (6)$$

The total channel gain of the NLOS path combining all  $\mathcal{K}$  squared surfaces of IRS is given by:

$$G_{\text{NLOS}} = \sum_{k=1}^{\mathcal{K}} G_{\text{NLOS}}^{\text{IRS}_k}(\gamma, \omega) \quad (7)$$

## 2.2. OWC systems with mirror array-based IRS

OWC with mirror array-based IRS has advanced rapidly in recent years. This surge in research interest and technological advancements highlights the potential of mirror array-based IRS to significantly enhance OWC systems. Table 3 summarizes the recent studies and key findings in this exciting field. In this section, we review the recent advancements in the application of mirror array-based IRS in OWC systems. Our review is categorized into four main areas, each representing a critical aspect of OWC system optimization: channel gain optimization, link reliability optimization, data rate optimization, and security optimization. This categorization helps to systematically explore the multifaceted benefits of mirror array-based IRS in enhancing the performance and reliability of OWC systems.

**Table 3.** Research progress in the OWC system based on mirror array IRS.

Year	Optical Source	Channel Type	Receiver	Optimization Objective	Optimization Algorithm	Comment	Ref.
2020	LD	Free Space	PD	Outage Probability	N/A	Dynamic Channel	[46,47]
2020	LED	Indoor	PD	Channel Gain	Author's Algorithm	Energy Efficient	[48]
2021	LED	Indoor	PD	Data Rate	Sine-Cosine Algorithm	N/A	[22]
2021	LED	Indoor	PD	Data Rate	Relaxing Greedy Algorithm	N/A	[49]
2021	LD	Free Space	PD	Outage Probability	N/A	Atmospheric turbulence	[18,42]
2021	LED	Indoor	PD	Secure	PSO Algorithm	N/A	[21]
2022	LD	Underwater	N/A	Outage Probability	N/A	Underwater turbulence	[50]
2022	LED	Indoor	PD	Channel Gain	Genetic Algorithm	NOMA	[45]
2022	LED	Indoor	PD	Channel Gain	MM Algorithm	SE maximization	[41]
2022	LED	Indoor	PD	Channel Gain	Cyclic Search Algorithm	MISO	[51]
2022	LED	Outdoor	PD	Channel Gain	BSCI Algorithm	V2V	[52]
2023	LD	Underwater	N/A	Outage Probability	N/A	Underwater turbulence	[53]
2023	LED	Indoor	PD	Channel Gain	N/A	FD Channel	[54]
2024	LED	Indoor	PD	Channel Gain	N-step localization Algorithm	VLP	[40]
2024	LED	Indoor	PD	Secure	PSO Algorithm	Multiple APs	[55]

Abbreviations: LD - Laser Diode; PD - Photodiode; LED - Light-Emitting Diode; PSO - Particle Swarm Optimization; NOMA - Non-orthogonal Multiple Access; MM - Minorization Maximization; SE - Spectral Efficiency; MISO - Multiple Input Single Output; BSCI - Binary Search Convergence Iterative; V2V - Vehicle to Vehicle; FD - Frequency Domain; VLP - Visible Light Positioning; AP - Access Point.

### 2.2.1. Channel Gain Optimization

Recent studies on the application of mirror array-based IRS in OWC systems can be broadly categorized into four main areas based on the major optimization target. The first major area focuses on optimizing the system's channel gain, to improve the overall performance and efficiency of OWC systems. In [48], it explores the enhancement of energy efficiency in a downlink RIS-assisted OWC system by simultaneously optimizing time allocation and power control. Unique to OWC systems,

constraints such as non-negative transmission signals and limited amplitude are introduced. The authors reformulate the problem by reducing the number of variables involved and propose an iterative algorithm to optimize the time allocation and power control. This study demonstrates through simulations that the proposed method outperforms the conventional interior point method, achieving an energy efficiency gain of up to 0.127 dB. In addition, channel gain optimization with IRSs in an OWC system with Non-Orthogonal Multiple Access (NOMA) has been investigated in [45]. Unlike conventional NOMA-based OWC systems where users' decoding order and power allocation are based on the corresponding LOS channel gain, IRS-assisted systems allow the total channel gain at the receiver to be manipulated by tuning the IRS. The authors propose a framework for jointly designing the NOMA decoding order, power allocation, and IRS reflection coefficients to enhance the Bit Error Rate (BER) performance. They show that this multi-dimensional optimization problem is NP-hard and propose an adaptive-restart Genetic Algorithm (GA) to solve it efficiently. The results demonstrate significant BER reduction, achieving more than 7 dB gain in the transmitted signal Signal-to-Noise Ratio (SNR) for a BER of  $10^{-2}$ , compared to scenarios without IRS or with IRS using fixed maximum reflection coefficients (i.e., all IRS reflection coefficients are set to one).

Moreover, [41] investigates the joint optimization of IRS configuration, power allocation, and user association in a Time Division Multiple Access (TDMA)-based OWC system under the point source assumption. It provides detailed channel models for both LOS and NLOS links and derives the instantaneous signal expression to maximize the Spectral Efficiency (SE). A binary IRS coefficient matrix is introduced to simplify the configuration process, an alternating optimization algorithm is proposed to maximize SE, and the variable frozen algorithm and Minorization-Maximization (MM) algorithm are used to address subproblems.

The MM algorithm is used in the reviewed studies to optimize the RIS. This algorithm constructs a surrogate function that approximates the original objective function and iteratively improves the solution. Specifically, the MM algorithm is applied to solve the power allocation problem with fixed parameters and Channel State Information (CSI) matrices.

The detailed steps of the MM algorithm in [41] for IRS optimization are as follows:

---

**Algorithm 1** MM Algorithm to Solve IRS Optimization Problem [41]

---

**Require:** Fixed parameters  $F, G$ , and  $\epsilon_2$ , and CSI matrices  $H^{(1)}$  and  $H^{(2)}$ .

**Ensure:** Suboptimal power allocation matrix  $P$ .

- 1: **Init:** Set iteration rounds  $t \leftarrow 0$ , and initialize  $x_1^{*(0)}, \eta(x_1^{*(0)}), \zeta(x_1^{*(0)})$ , and  $x_2^{*(0)}$ .
- 2: **repeat**
- 3:    $t \leftarrow t + 1, k \leftarrow 1$ ;
- 4:   Solve subproblem (P2-a) using the Proximal Gradient Descent (PGD) algorithm and find the power allocation matrix  $P^{(t)}$ ;
- 5:   **repeat**
- 6:     Update  $x_1^{*(t)} \leftarrow w\gamma_k(P^{(t)})$ ;
- 7:     Calculate  $\eta(x_1^{*(t)})$  based on (38);
- 8:     Calculate  $\zeta(x_1^{*(t)})$  based on (39);
- 9:     Update  $x_2^{*(t)} \leftarrow \sigma_k^2 + \rho_k^2 \sum_{i=1, i \neq k}^K (h_k^{(1)T} P^{(t)} f_i)^2$ ;
- 10:     $k \leftarrow k + 1$ ;
- 11:    **until**  $k > K$ ;
- 12:   **until**  $\|P^{(t+1)} - P^{(t)}\|_F < \epsilon_2$
- 13: **Set**  $P^* \leftarrow P^{(t)}$ .

---

Thanks to the MM algorithm, the SE has been significantly improved, achieving a nearly linear SE gain with respect to the number of IRS units and reflection factors. Additionally, the impact of geometric factors on IRS performance is highlighted, providing a detailed analysis of IRS locations and room sizes [41].

Previous papers have primarily focused on Single-Input-Single-Output (SISO) OWC systems. SISO systems often struggle with limited robustness, particularly against channel blocking, which can significantly impact their performance in high-capacity applications. To address these limitations, [51] investigates a RIS-assisted Multiple-Input-Single-Output (MISO) OWC system with a focus on channel gain improvements. The authors model the mirror array-based RIS-aided MISO-OWC channel shown

in Figure 2 and formulate an optimization problem to reconfigure the direction of each RIS element. The goal is to maximize the asymptotic capacity at high SNR for the system employing Intensity Modulation/Direct Detection (IM/DD) with peak-power constraints. The non-convex optimization problem is converted into a Quadratic Programming (QP) problem with hemispherical constraints, which can be solved by calculating the maximum eigenvalue of an equivalent matrix. Simulation results show that the asymptotic capacity of the MISO-OWC channel improves with RIS, with the NLOS channel gain increasing significantly as the number of mirrors increases. Specifically, when the number of mirrors increases from 15 to 1500, the NLOS channel gain increases from 0.09 to 0.22. The study also examines the impact of the distance between the receiver and RIS, showing that closer proximity results in greater performance improvement, achieving up to a 35% capacity gain compared to systems without RIS.

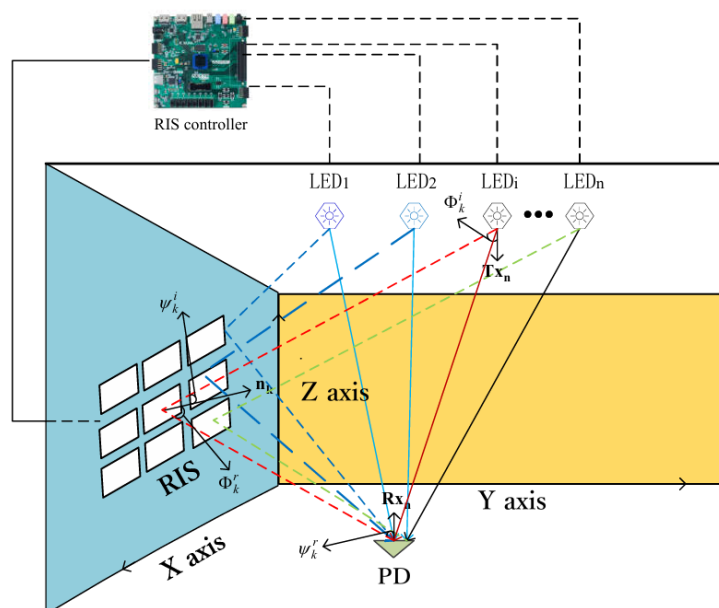


Figure 2. RIS-aided indoor MISO-OWC system [51].

While prior research has predominantly centered on using IRS in indoor OWC systems, [52] extends the application of IRS-based OWC to Vehicle-to-Vehicle (V2V) communication. It studies the effect of the number of IRS elements on the Energy Efficiency (EE) in an OWC system for parallel vehicles. The authors design a system with the transmitter on the right headlamp of one vehicle, the receiver between the headlamps of another, and the IRS on a streetlight pole shown in Figure 3. The achievable rate and power consumption are analyzed under different numbers of IRS mirror elements. An optimization problem for maximizing the EE is formulated, and the Binary Search-Conditional Iterative (BSCI) algorithm, which iteratively calculates a range and uses binary search to find the optimal solution, is proposed to efficiently find the optimal number of elements. Simulation results demonstrate that the proposed method significantly improves EE, using only a small fraction of the total mirrors available and requiring minimal computational effort compared to traditional methods.

**Algorithm 2** BSCI Algorithm [52]

---

**Require:** Parameter values for the system components (e.g., LED, PD, IRS), initial iterative range  $N_{\min}$  and  $N_{\max}$ , formulas for calculating the range and objective function.

**Ensure:** Optimal value  $N_{\text{opt}}$  and maximum objective  $EE_{\max}$ .

- 1: Calculate the iterative range  $N$  based on the provided parameters.
- 2: Calculate  $R(N)$  using the iterative range  $N$ .
- 3: **for**  $N = N_{\min}$  to  $N_{\max}$  **do**
- 4:   Calculate  $EE(N)$  based on the objective function.
- 5:   **if**  $EE(N) < EE(N-1)$  **then**
- 6:      $N_{\text{opt}}$  does not exist;
- 7:     **break**;
- 8:   **else if**  $EE(N) \geq EE(N-1)$  **then**
- 9:      $N_{\text{opt}} = N$ ;
- 10:     $EE_{\max} = EE(N)$ ;
- 11:   **end if**
- 12: **end for**
- 13: Use the binary search method to refine  $N_{\text{opt}}$  and  $EE_{\max}$ .
- 14: **Output**  $N_{\text{opt}}$  and  $EE_{\max}$ .

---

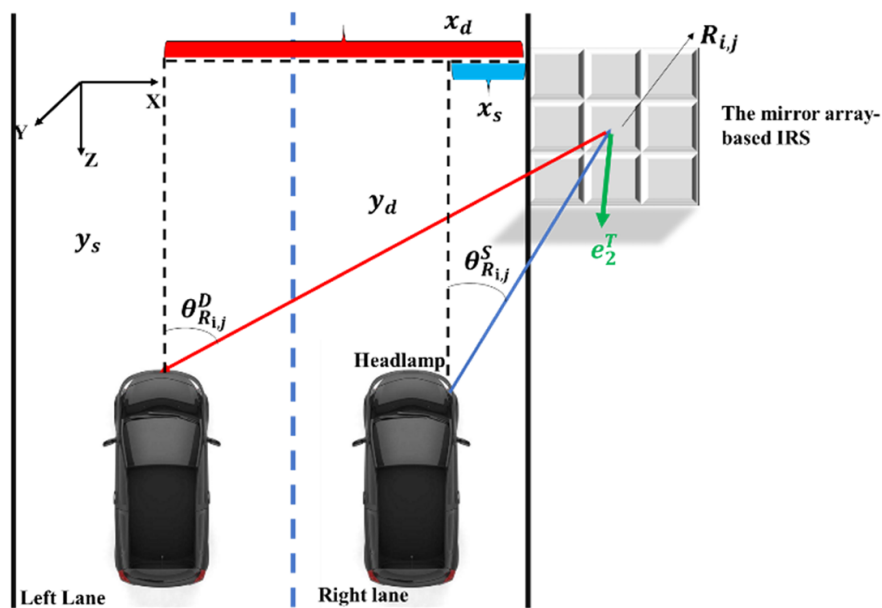


**Figure 3.** Model of the OWC system via mirror array-based IRS for parallel vehicles [52].

Unlike previous studies that have focused on time-domain characteristics, [54] investigates the Frequency-Domain (FD) channel characteristics of IRS-assisted OWC systems. A comprehensive tapped-delay line channel model for IRS-assisted OWC systems is proposed, and the frequency-selective channel characteristics due to IRS-induced time delay are validated through experiments. Key findings indicate that the IRS array enhances OWC system performance when it operates as a narrowband system or when the strength of the reflected channel via the IRS array is significantly larger than the LOS channel. In wideband OWC systems, however, similar or worse performance compared to the LOS-only case is observed. The study also presents an achievable rate analysis using Direct Current-biased Optical Orthogonal Frequency-Division Multiplexing (DCO-OFDM), deriving a closed-form expression for the achievable rate. The results show that with a path loss ratio of zero, the achievable rate is 2.86 Gbps. Increasing the path loss ratio to two raises the achievable rate to over 4 Gbps. In scenarios where the IRS reflected signal is stronger than the LOS path, the achievable rate consistently improves. The channel gain measurements in various configurations exhibit low-pass characteristics due to the limited bandwidths of optical front-ends, with systems incorporating both LoS and IRS paths showing greater frequency fluctuations. These findings imply that IRS activation should be channel-dependent or require a gain control mechanism.

In addition to performance improvements in OWC systems, IRS also offers valuable benefits for optical wireless-based positioning systems, such as Visible Light Positioning (VLP) systems. In [40], the authors investigate a VLP system where an OWC receiver with a single photo-detector estimates its position using Received Signal Strength (RSS) measurements from multiple LED transmitters, including signals from both LOS and reflected paths via IRSs. The study's main contributions include developing an achievable Cramer-Rao Lower Bound (ACRLB) expression for the 3D positioning accuracy, proposing a Maximum Likelihood (ML) estimator for position estimation, and optimizing IRS orientation when LOS paths are blocked. Additionally, an N-step localization algorithm, which iteratively refines the estimated position through multiple steps leveraging different IRS configurations, is introduced to improve positioning accuracy. The results show that the Root Mean Square Error (RMSE) of the ML estimator can be reduced to 4.2 cm with optimized IRS configurations, compared to 27.5 cm with the lowest noise variance and standard configurations. Extensive simulations demonstrate the impact of IRS parameters and LOS path blockages on positioning accuracy, showing that while IRSs offer limited improvements in the presence of sufficient LOS signals, they are crucial for accurate positioning when LOS paths are obstructed.

### 2.2.2. Link Reliability Optimization

Having explored the role of IRS in optimizing the channel gain and positioning accuracy in OWC systems, IRS-based OWC systems have also been widely studied with a focus on link reliability optimization. [46,47] presents a comprehensive analysis of FSO systems assisted by IRS, focusing on improving link reliability by reducing the outage probability. Unlike previous studies, this work incorporates pointing errors, IRS plane jitter, and obstruction of obstacles in the performance evaluation. Key contributions include deriving closed-form expressions for SISO and SIMO IRS-assisted systems, proposing a multi-branch IRS-assisted system adaptable to environments with obstacles, and providing asymptotic Probability Density Function (PDF) and Cumulative Distribution Function (CDF) expressions for IRS channel coefficients. The study also develops an optimal power allocation scheme and demonstrates the system performance gains with increasing intelligent channels. Numerical results validate the accuracy of the derived expressions and highlight the impact of system parameters on BER and outage probability. Specifically, it is shown that with a transmission power of 30 dBm, the outage probability is reduced from  $10^{-2}$  to  $10^{-5}$  with the assistance of IRS. Similarly, [18,42] investigate the use of IRS to optimize link reliability in FSO systems. The authors first specify the phase-shift distribution across the IRS for desired beam reflection, demonstrating an equivalence to a mirror-assisted FSO system. They derive Geometric and Misalignment Loss (GML) as a function of IRS characteristics and develop statistical channel models accounting for the impact of building sway on the transmitter, receiver, and IRS. The models are applicable to both 2D and 3D systems and include outage probability analysis considering atmospheric turbulence. Simulations validate the models and provide key insights for IRS-assisted FSO systems design. For instance, with a 10 cm IRS for a 1 km link, beam truncation is negligible. Additionally, the analysis of outage probability shows that identical position variances of the transmitter, IRS, and receiver affect the channel differently, depending on their relative positions.

While the aforementioned studies focus on enhancing link reliability in FSO systems, IRS technology can also be effectively applied to Underwater Optical Wireless Communication (UOWC) systems to achieve similar improvements. In [50], an IRS-assisted UOWC system was proposed to overcome signal losses in underwater environments caused by obstructions like aquatic plants, underwater vehicles, seamounts, and environmental conditions such as turbidity and salinity. These factors can cause significant burst errors and random errors in UOWC systems. The study characterizes the IRS-assisted UOWC channel by combining underwater turbulence models, beam attenuation, occlusion due to obstacles, and pointing errors. It derives the PDF and CDF expressions for the SNR in a system with  $N$  IRS elements. Analytical expressions for outage probability are also derived and validated through Monte Carlo simulations. The results demonstrate that IRS can significantly reduce

the outage probability; for example, at an average SNR of 40 dB, a system with 16 IRS elements can reduce the outage probability from  $0.9 \times 10^{-2}$  to  $0.8 \times 10^{-3}$ . Moreover, in [53], the authors investigate the outage probability performance of IRS-assisted UOWC links, considering the effects of attenuation, pointing errors, and turbulence. Unlike [50], which focuses on the combined impact of occlusion and environmental factors, this study specifically models the underwater turbulent medium using the Oceanic Turbulence Optical Power Spectrum (OTOPS) model, which incorporates practical values for average temperature and salinity concentration in earth basins. The study finds that integrating IRSs into the underwater medium significantly enhances link reliability under various adverse conditions. Notably, the results show that without IRS, the average BER is approximately  $7 \times 10^{-3}$ . However, with the addition of IRS elements, the outage probability decreases dramatically: to  $1.5 \times 10^{-4}$  with 20 IRS elements,  $1.9 \times 10^{-5}$  with 100 IRS elements, and further to  $2.4 \times 10^{-6}$  and  $9.9 \times 10^{-7}$  with 500 and 1000 IRS elements, respectively. This substantial improvement shows the potential of IRS technology in mitigating signal loss and enhancing communication reliability in challenging underwater environments.

### 2.2.3. Data Rate Optimization

In addition to optimizing the channel gain and link reliability in OWC systems, IRS has also been studied for enhancing data rates in these systems. In [22], an IRS-aided indoor OWC system is proposed to address the LOS blockage problem while accounting for random receiver orientations. This study is the first to quantitatively explore the use of IRSs to enhance data rates and improve system reliability in the absence of an LOS path. The authors develop an optimization problem to configure the orientation of IRS elements to maximize the achievable rate. Due to the non-convex nature of the problem, a sine-cosine-based optimization algorithm is introduced, which is designed to solve complex optimization problems by using cooperative and competitive search agents and finding the global optimal solution. Simulation results demonstrate significant improvements in data rate and outage performance, with the proposed design achieving up to 397% improvement in data rate and 50% reduction in outage compared to wall-only reflections. The study also highlights the impact of the number of blockers on system performance and confirms that the IRS-aided system outperforms no-IRS systems by up to 28.84% in data rate across various scenarios.

In addition, in [49], the authors consider an IRS-aided OWC system that includes both NLOS paths specularly reflected by the IRS and LOS paths. Unlike previous methods that focused on optimizing mirror orientation, this study leverages the high spatial resolution of specular reflection paths and introduces a discrete matrix to represent the association between LEDs and IRS units. The IRS allocation is formulated as a binary programming problem. By pre-mapping IRS unit coefficients to emergence angles using a look-up table, the coefficients can be efficiently found using a reverse look-up table. A relaxing greedy algorithm, which iteratively improves the solution by selecting the best option at each step and relaxing constraints when necessary, is proposed to solve this binary programming problem, with the achievable sum rate as the evaluation metric. Complexity analysis and numerical results show that the proposed algorithm significantly reduces computational complexity compared to brute force methods and performs well even with many users. Results indicate that using 256 IRS units can improve the achievable sum rate by nearly 12 Megabits per Second (Mbps) in high SNR regimes, outperforming random selection and distance-based methods, with an additional gain of about 2 Mbps over the distance greedy method. The base data rate without IRS units and under shadowing conditions is approximately 5 Mbps.

### 2.2.4. Security Optimization

In addition to enhancing the channel gain, link reliability, and data rate, IRS technology also holds significant promise for optimizing security in OWC systems. In [21], the authors propose an IRS-aided OWC system to enhance the secrecy performance. They model the reflected channel gain in an OWC system using an intelligent controllable mirror array as IRS and derive a lower bound on the achievable

secrecy rate for the IRS-aided peak power-constrained OWC system employing IM/DD. The study focuses on optimizing mirror orientations to maximize the difference between the channel gains of the legitimate user and the eavesdropper. The orientation optimization problem is transformed into a reflected spot position-finding problem, significantly reducing complexity. Simulation results show that, without the IRS, the LOS channel gains of both legitimate users and eavesdroppers vary similarly. Specifically, when eavesdroppers are close to legitimate users, the channel gain difference decreases from 0.05 to 0 and remains close to 0 over a large range of approximately 1.6 meters, resulting in limited secrecy rates and large insecure areas. With the IRS, the sum channel gain difference is significantly enlarged, leading to improved secrecy rates. Specifically, when using the IRS, the sum channel gain difference decreases from approximately 0.19 to 0, which only occurs when the eavesdropper is very close to the legitimate user. This critical distance is only 0.2 meters, compared to 1.6 meters without the IRS, showing a significant reduction in insecure areas. This results in a larger difference in the sum channel gain between the legitimate user and the eavesdropper, thereby enhancing the achievable secrecy rate.

Similarly, in [55], the authors study a mirror array IRS-aided secure OWC system with multiple transmitters and several independent two-dimensional rotatable mirror elements located at different positions. The goal is to create an optimal reflecting environment through mirror array IRS rotation control, enhancing legitimate user transmission while restricting eavesdropper reception. The study provides a closed-form expression of the achievable secrecy rate as a function of mirror orientations and AP-mirror element association. The optimization problem to maximize the secrecy rate is handled by a Reflected Spot Search (RSS) transformation method, which simplifies and splits the problem into subproblems. These subproblems are solved using an improved Particle Swarm Optimization (PSO) algorithm and a traverse-like method. Additionally, the dual task of communication and illumination is considered, with analysis of illumination uniformity. Simulation results show that the proposed RSS method achieves better secrecy performance than other IRS configuration methods with minimal impact on illumination uniformity. For instance, the results indicate that the legitimate user's IRS gain is positive and close to his LOS gain, while the eavesdropper's IRS gain remains zero unless their positions overlap. The simulation results are very similar to the previous study [21]. When eavesdroppers are close to legitimate users, the channel gain difference decreases from 0.05 to 0 and remains close to 0 over a large range of approximately 1.6 meters without IRS. However, with IRS, the sum channel gain difference decreases from approximately 0.6 to 0, which only occurs when the eavesdropper is very close to the legitimate user. This critical distance is only 0.2 meters, compared to 1.6 meters without the IRS, showing a significant reduction in insecure areas. Notably, the main difference between the two studies is that the sum channel gain difference is significantly enhanced when using IRS. These subproblems are solved using an improved PSO algorithm and a traverse-like method.

### 3. Metasurface-Based IRS in OWC Systems

In addition to mirror array-based IRS, metasurface-based IRS also offers significant potential for enhancing OWC systems. Metasurfaces consist of engineered materials with sub-wavelength structures that can manipulate light waves in highly controlled ways. These structures can modify various properties of the incident light, such as phase, amplitude, and polarization [56], leading to improved signal propagation, interference mitigation, and system performance.

In OWC systems, mirror array-based IRS primarily relies on the reflection of light, and metasurface-based IRS not only reflects signal light but can also be applied to refract signal light. Both metasurface IRS and mirror array IRS can be positioned between the transmitter and receiver to utilize the reflective properties of light for signal redirection. Metasurface IRS further extends its functionality by employing refractive properties, allowing for advanced signal beam shaping [57,58] and control of the receiver's FOV [28,59]. This versatility enables metasurface IRS to be placed not only between the transmitter and receiver but also directly at the transmitter for beam shaping and at the receiver for

signal concentration. This dual capability of controlling light through both reflection and refraction provides metasurface IRS with a distinct advantage in optimizing OWC system performance across various deployment scenarios.

### 3.1. Signal Reflection with Metasurface-based IRS

Recent research has begun to explore the potential of metasurface-based IRS to enhance OWC systems through signal reflection. While the number of studies investigating this approach is relatively limited, here we review some of the latest papers focusing on the implementation and benefits. The study [60] demonstrates a multifunctional electro-optically tunable metasurface for NIR wavelengths. This metasurface can dynamically control the phase profile of reflected light as shown in Figure 4, enabling functions such as beam steering and focusing at different focal lengths (1.5, 2, and 3  $\mu\text{m}$ ) by adjusting the applied bias voltage. The spatial distribution of the phase shift was designed to achieve precise control of the reflected beam, showcasing the potential for enhancing optical wireless communication systems through intelligent signal manipulation.

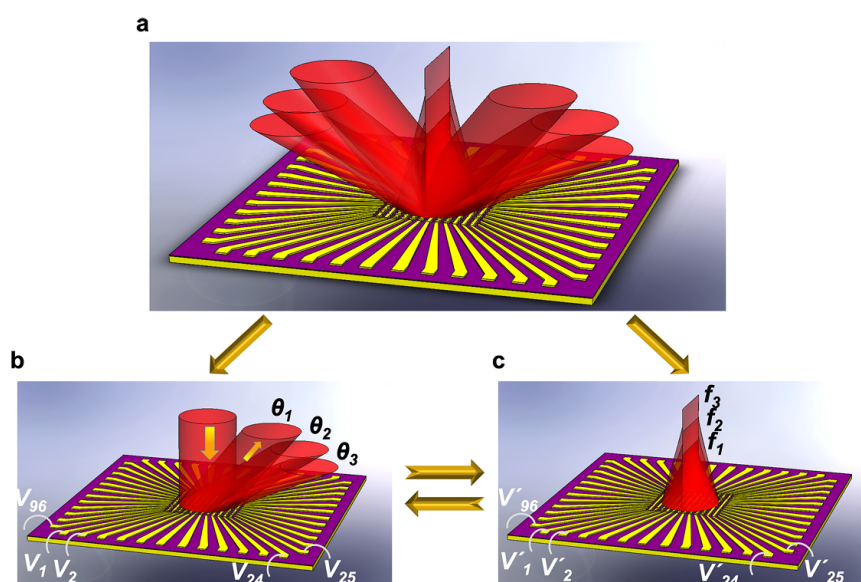


**Figure 4.** Illustration of a multifunctional metasurface composed of 96 independently addressable elements. The metasurface can switch functions between (b) dynamic beam steering and (c) cylindrical metalens with reconfigurable focal length [60].

Moreover, [61] presents an ultracompact full-duplex OWC system using a dielectric beam-steering metasurface, manufactured using CMOS processes for mass production and integration with other optoelectronic components as shown in Figure 5. The system supports Point-to-Multipoint (PtMP) downlink broadcasting and uplink data transmission for each user. The metasurface achieves dynamic beam steering by changing the polarization of incident light, achieving a downstream capacity of up to 100 Gbps with a large beam-steering angle of  $\pm 40^\circ$ . Up to 14 user channels can be supported and 10 Gbps upstream is achieved per user channel. Experimental results show that the power loss fluctuation for ten wavelengths at three different polarization states is less than 1.6 dB, demonstrating the system's flexibility and stability, and highlighting its potential for large-scale commercial applications.

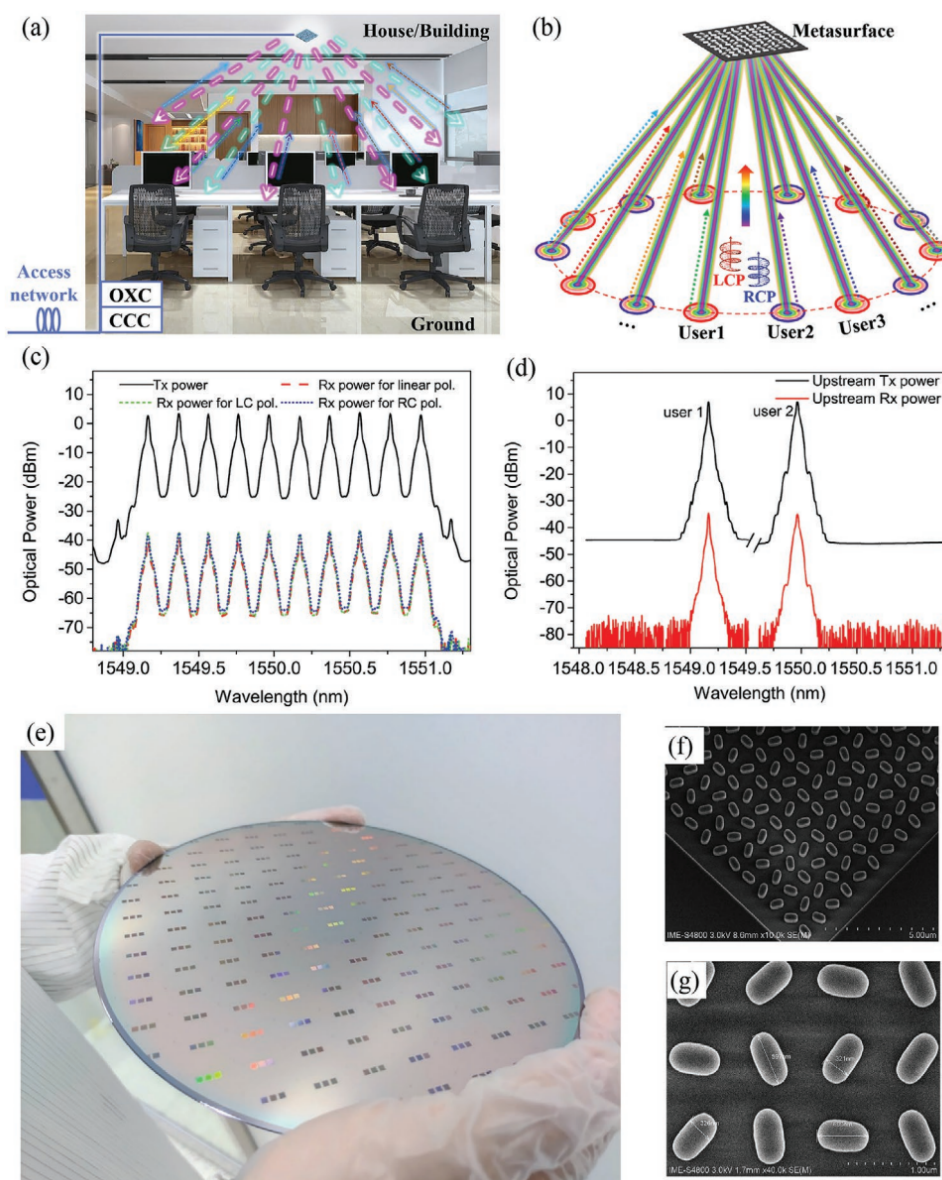


**Figure 5.** Overview of a full-duplex optical wireless broadcasting system utilizing beam-steering metasurfaces, along with experimental results and manufacturing details [61].

In addition, [24] systematically compares the performance and applications of mirror array IRS and metasurface IRS in OWC systems. The authors propose an analytical framework to study the capabilities of adaptive metasurfaces and mirror array-based reflectors in directing radiated power toward a specific detector. They derive the phase gradients for metasurface arrays and the orientation of mirror array elements needed to focus the incident power onto the detector center. Expressions for irradiance on the detector plane for both reflector types are provided, along with a new metric to evaluate reflectors' performance based on the received power. The study quantifies the received power gain compared to LOS scenarios and examines the impact of the number of reflecting elements and detector location through simulations. The findings reveal that using different types of IRS (mirror array and metasurfaces) can significantly increase the received optical power. Specifically, the reflectors' gain performance compared to the LOS link can achieve a factor of 30 in most areas under different positions of the two types of IRS. The mirror array maintains received power gains better at smaller distances, while the metasurface's performance degrades as the detector gets closer. However, the mirror array's superiority decreases with increasing distance between the reflector and the receiver.

### 3.2. Signal Refraction with Metasurface-based IRS

In addition to the light reflection capability, metasurface-based IRS can also manipulate light through refraction, providing a powerful tool for enhancing OWC systems. Metasurfaces can achieve precise control over the spatial phase and polarization of incident light, allowing for advanced signal beam shaping and redirection. The refraction capability enables metasurface-based IRS to be placed at various points in the communication link, including at the transmitter for beam shaping and at the receiver for signal concentration, thereby optimizing the FOV and improving overall system performance. This section summarizes recent advancements in using refraction-based metasurface IRS in OWC systems.

#### 3.2.1. Beam Shaping with Metasurface IRS

Placing metasurface-based IRS at the transmitter end allows for beam shaping [62,63], enabling the transmitted signal to be directed in a highly controlled manner. This approach can enhance the directivity of the signal, reduce interference [23], and ensure that the optical power is concentrated towards the intended receiver [64], thereby improving the efficiency and reliability of the communication link. In [65], the authors propose an adaptive UOWC link using multi-wavelength lasers and an ultra-broadband metasurface for converting Gaussian beams to Circular Auto-Focusing Airy Beams (CAFAB). The metasurface demonstrates uniform conversion efficiency across the visible light spectrum, enhancing beam propagation and mitigating occlusions. The study evaluates the performance of Red, Green, and Blue (RGB) CAFAB lasers in UOWC scenarios, highlighting their ability to maintain reliable, high-speed, and long-range communication even in the presence of underwater obstacles and air bubbles. Experimental results show that the proposed RGB Airy beam-based UOWC system outperforms traditional Gaussian beam systems. Specifically, when the obstacle diameter is  $0.43 \omega_0$  (where  $\omega_0$  is normalized to a maximum transmitter beam aperture of approximately 14 mm), the RGB Airy beam system achieves a data rate that is 7.3 Gbps higher than the RGB Gaussian beam system and 17.8 Gbps higher than the single blue laser Gaussian beam-based link. The Received Optical Power (ROP) for RGB channels with the metasurface is significantly higher compared to channels without the metasurface. Specifically, the red channel shows a 3.4 dB ROP improvement, while the green and blue channels demonstrate enhancements of 9.66 dB and 4.74 dB, respectively. Additionally, the data rate of RGB Airy beams remains superior even as the obstacle size increases, demonstrating the potential of IRS for robust UOWC transmission in challenging environments.

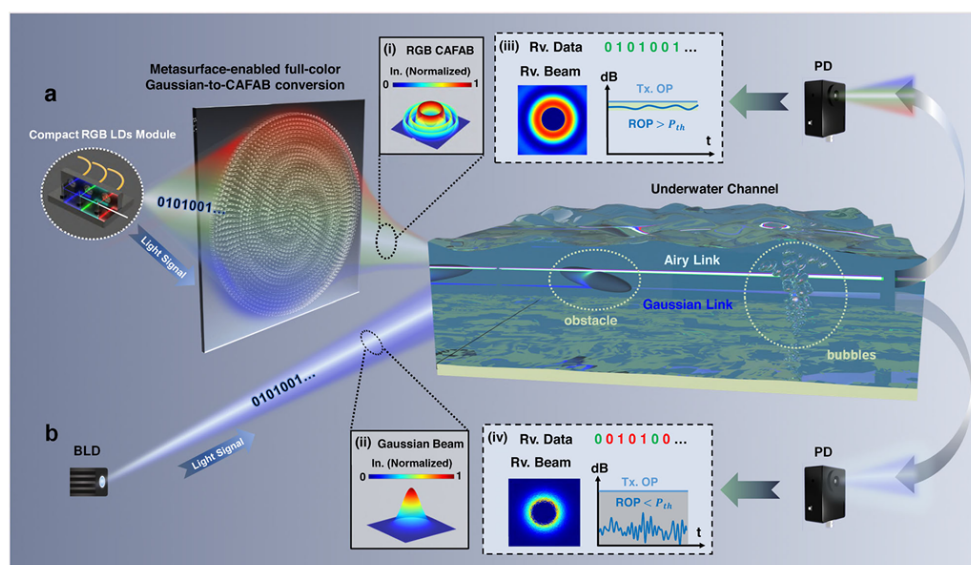


**Figure 6.** Schematics illustrating (a) a conventional Gaussian beam-based UOWC system and (b) our adaptive link using multi-wavelength Airy beams transformed by an ultra-broadband metasurface. The compact LDs module generates tri-color Gaussian beams, which are converted to circular Airy beams by a metasurface for a Wavelength-Division Multiplexing (WDM) scheme. Insets (i) and (ii) show intensity profiles of CAFAB and Gaussian beams, respectively, while (iii) and (iv) depict received information for link a and link b. Traditional UOWC links typically use blue Gaussian beams, with performance affected by underwater conditions [65].

In addition, in [58], a fluid-infiltrated, multifunctional, all-dielectric metasurface platform was designed to enhance the OWC network performance by addressing tunability issues for optimal communication efficiency. The metasurface is experimentally demonstrated to provide simultaneous connectivity to multiple users and becomes a tunable varifocal device when infiltrated with different fluids. Numerical simulations and experimental validations show that the metasurface can effectively provide on-demand connectivity and directivity improvements. By manipulating the fluid's refractive indices, the metasurface can dynamically adjust its focal length, thus enabling precise beam shaping to enhance signal direction and focus. Characterization using fluids with varying refractive indices confirmed the device's functionality, achieving a focusing efficiency of approximately 18% for both left and right circularly polarized incident light. Focusing efficiency refers to the proportion of incident light energy that is successfully concentrated at the desired focal point by the metasurface. This metric is crucial for evaluating the effectiveness of the metasurface in directing and concentrating light, which is essential for applications such as optical wireless communication. This fluid-responsive metasurface offers enhanced adaptability, improved signal directivity, and increased data transfer efficiency compared to conventional methods.

Furthermore, in [57], a polarization-insensitive beam-steering metasurface was employed in a bidirectional coherent OWC system. This system achieved 100 Gbps real-time Dual-Polarization Quadrature Phase Shift Keying (DP-QPSK) signal distribution to 9 users over a 2 m distance without the need for Erbium-Doped Fiber Amplifiers (EDFAs) or optical filters at the reception side. The metasurface's beam-steering capability allows for precise control of the beam direction, enabling efficient signal distribution to multiple users. The metasurface had a Polarization-Dependent Loss (PDL) of less than 1.2 dB, and all users maintained BERs below the soft decision Forward Error Correction (FEC) limit of  $2.4 \times 10^{-2}$ . This integration of optical coherent communication with metasurface technology reduces system complexity and cost while ensuring high data rates, rendering it a promising solution for future high-performance wireless communications. The ability to steer the beam accurately ensures that the signal is directed where it is most needed, enhancing the overall system efficiency and user experience.

### 3.2.2. FOV Enhancement with Metasurface IRS

Positioning metasurface-based IRS at the receiver end increases the receiver's sensitivity to incoming signals, mitigates alignment issues, and enhances the overall robustness of the OWC system by concentrating the received optical power. In [28], a novel Liquid Crystal (LC) IRS-based receiver was designed to enhance the signal strength and data rate without using power amplifiers. The LC IRS can steer the incident light within the PD's FOV by adjusting its refractive index. Simulation results show that the LC IRS-based receiver can achieve up to 731%, 688%, and 591% improvement in data rates for light wavelengths of 510 nm, 550 nm, and 670 nm, respectively, compared to ordinary receivers. The proposed optimization algorithm outperforms benchmark schemes and achieves optimal performance in fewer iterations. The study also highlights the importance of maintaining the incident angle below  $60^\circ$  to ensure higher transition coefficients and better overall channel gain.

Furthermore, in [59], the authors explore the use of two types of intelligent meta-elements to steer incident light beams at the receiver in OWC systems: a meta-lens with electrically stretchable artificial muscles and a liquid-crystal-based IRS with an adjustable refractive index. These innovative elements can replace traditional lenses, offering advantages such as a large incident angle, and allowing the receiver to detect signals while rotating. The study demonstrates that using IRS elements significantly improves signal detection capabilities by increasing the receiver's FOV. The study demonstrates that the performance of an IRS element in OWC systems is significantly influenced by the incidence angle, physical depth, and tuning gain, all of which influence the FOV. The transmittance of the IRS decreases with an increase in the incidence angle, while the refracted light intensity increases as the angle decreases. Around a wavelength of 600 nm, an IRS with a 0.2 mm physical depth can completely absorb incoming light, whereas increasing the depth to 0.8 mm reduces this absorption by about 90%, delivering nearly all the light intensity to the PD. Additionally, the tuning gain, which varies with the IRS physical depth and wavelength, indicates significant intensity gains from the tuning operation. These findings underscore the potential of metasurface IRS in significantly improving the FOV and enhancing OWC system performance.

## 4. Conclusions and Future Scope

This survey discusses two types of IRS in OWC systems, each with its own advantages and limitations. Mirror array-based IRS has shown effectiveness in reflecting incident light to enhance communication performance, addressing challenges such as signal blockage and interference mitigation. Studies have demonstrated significant improvements in channel gain and data rate, particularly in indoor OWC systems and V2V communication scenarios. Additionally, mirror array-based IRS can enhance link reliability by reducing outage probability, even in complex environments with significant physical obstructions. Due to mirror array-based IRS relying primarily on signal reflection, they have a simple structure and easy deployment. However, its limitation lies in its inability to manipulate the amplitude of light, being restricted to altering only the spatial phase or direction of the light path. Additionally, mirror array-based IRS can only be placed within the communication channel.

Metasurface-based IRS offers further advantages by not only reflecting light but also manipulating it through refraction, due to the metasurface-based IRS rooted in new meta-materials. This capability can manipulate the phase, amplitude, and direction of the incident light, enabling advanced signal beam shaping and focusing, enhancing the FOV, and improving overall system performance. The ability to place metasurface IRS at various points in the communication link, including the transmitter and receiver, provides flexibility in system design and optimization. However, its complexity and dependence on material advancements pose major challenges.

Recent studies have leveraged various algorithms to control the IRS for optimal system performance, often based on static system models. However, real-world systems are dynamic, influenced by factors such as human movement in indoor OWC systems, weather changes, and turbulence in FSO systems. Thus, the ability to dynamically adjust and control IRS in response to environmental changes is crucial.

Conventional feedback methods typically rely on pre-defined models and periodic measurements, which can be inadequate in rapidly changing environments. Machine Learning-based methods offer a more dynamic alternative, capable of predicting and adapting to environmental variations using real-time data. However, Machine Learning approaches require significant data, and computational resources, and can introduce processing latency. Effective feedback control requires timely and accurate data acquisition about the channel conditions. This can be achieved through integrated sensors or external devices, ensuring low-latency communication with the IRS. Machine Learning methods, while powerful, necessitate substantial computational resources and efficient algorithms to manage data processing in real-time.

Moreover, dynamic environments present significant challenges for channel modeling with IRS in OWC systems. Moving objects, varying weather conditions, and atmospheric turbulence can alter channel characteristics. Developing adaptive channel models that can predict and respond to these changes is essential. Hence, advancing feedback mechanisms, exploring Machine Learning-based approaches, optimizing data acquisition, and addressing channel modeling challenges are crucial for the future development of IRS-OWC systems.

In conclusion, the integration of IRS in OWC systems holds significant promise for enhancing communication performance across various metrics. Both mirror array-based and metasurface-based IRS have demonstrated their potential in optimizing channel gain, link reliability, data rate, and security. Ongoing research and development, particularly in dynamic control and feedback mechanisms, are crucial for realizing the full potential of IRS technology in future OWC systems.

**Conflicts of Interest:** The authors declare no conflicts of interest.

## Abbreviations

The following abbreviations are used in this manuscript:

ACRLB	Achievable Cramer-Rao Lower Bound
AP	Access Point
B5G	Beyond Fifth-Generation
BER	Bit Error Rate
BSCI	Binary Search Conditional Iterative
CAFAB	Circular Auto-Focusing Airy Beams
CCC	Communication Control Center
CDF	Cumulative Distribution Function
CMOS	Complementary Metal-Oxide-Semiconductor
CSI	Channel State Information
DCO-OFDM	Direct Current-biased Optical Orthogonal Frequency-Division Multiplexing
DP-QPSK	Dual-Polarization Quadrature Phase Shift Keying
EE	Energy Efficiency
EDFAs	Erbium-Doped Fiber Amplifiers
FD	Frequency-Domain
FEC	Forward Error Correction
FOV	Field of View
FSO	Free Space Optics
GA	Genetic Algorithm
Gbps	Gigabits per Second

GML	Geometric and Misalignment Loss
IM/DD	Intensity Modulation/Direct Detection
IRS	Intelligent Reflecting Surfaces
LC	Liquid Crystal
LCP	Left-Handed Circularly Polarized
LD	Laser Diode
LED	Light-Emitting Diode
LP	Linearly Polarized
LOS	Line-of-Sight
MEC	Mobile Edge Computing
MEMS	Micro-Electromechanical Systems
MIMO	Multiple-Input-Multiple-Output
MISO	Multiple-Input-Single-Output
ML	Maximum Likelihood
MM	Minorization-Maximization
mmWave	Millimeter-Wave
NLOS	Non-Line-of-Sight
NOMA	Non-Orthogonal Multiple Access
OTOPS	Oceanic Turbulence Optical Power Spectrum
OWC	Optical Wireless Communication
OXC	Optical Cross Connector
PD	Photodiode
PDF	Probability Density Function
PDL	Polarization-Dependent Loss
PIN	Positive-Intrinsic-Negative
PSO	Particle Swarm Optimization
PtMP	Point-to-Multipoint
QOS	Quality of Service
QP	Quadratic Programming
RCP	Right-Handed Circularly Polarized
RF	Radio Frequency
RGB	Red, Green, and Blue
RMSE	Root Mean Square Error
ROP	Received Optical Power
RSS	Reflected Spot Search
RSS	Received Signal Strength
SE	Spectral Efficiency
SEM	Scanning Electron Microscope
SISO	Single-Input-Single-Output
SNR	Signal-to-Noise Ratio
SOI	Silicon-On-Insulator
Tbps	Terabits per Second
TDMA	Time Division Multiple Access
THz	Terahertz
UAV	Unmanned Aerial Vehicles
UOWC	Underwater Optical Wireless Communication
V2V	Vehicle-to-Vehicle
VLC	Visible Light Communication
VLP	Visible Light Positioning
WDM	Wavelength-Division Multiplexing

## References

1. Wang, K.; Song, T.; Wang, Y.; Fang, C.; He, J.; Nirmalathas, A.; Lim, C.; Wong, E.; Kandeepan, S. Evolution of Short-Range Optical Wireless Communications. *Journal of Lightwave Technology* **2023**, *41*, 1019–1040. <https://doi.org/10.1109/JLT.2022.3215590>.
2. Khalighi, M.A.; Uysal, M. Survey on free space optical communication: A communication theory perspective. *IEEE communications surveys & tutorials* **2014**, *16*, 2231–2258.
3. Koonen, T. Indoor optical wireless systems: technology, trends, and applications. *Journal of Lightwave Technology* **2017**, *36*, 1459–1467.
4. Aboagye, S.; Ndjiongue, A.R.; Ngatched, T.M.N.; Dobre, O.A.; Poor, H.V. RIS-Assisted Visible Light Communication Systems: A Tutorial. *IEEE Communications Surveys & Tutorials* **2023**, *25*, 251–288. <https://doi.org/10.1109/COMST.2022.3225859>.
5. Niu, Y.; Li, Y.; Jin, D.; Su, L.; Vasilakos, A.V. A survey of millimeter wave communications (mmWave) for 5G: opportunities and challenges. *Wireless networks* **2015**, *21*, 2657–2676.
6. Koenig, S.; Lopez-Diaz, D.; Antes, J.; Boes, F.; Henneberger, R.; Leuther, A.; Tessmann, A.; Schmogrow, R.; Hillerkuss, D.; Palmer, R.; et al. Wireless sub-THz communication system with high data rate. *Nature photonics* **2013**, *7*, 977–981.
7. Chen, Z.; Ma, X.; Zhang, B.; Zhang, Y.; Niu, Z.; Kuang, N.; Chen, W.; Li, L.; Li, S. A survey on terahertz communications. *China Communications* **2019**, *16*, 1–35.
8. Alimi, I.; Shahpari, A.; Sousa, A.; Ferreira, R.; Monteiro, P.; Teixeira, A.; et al. Challenges and opportunities of optical wireless communication technologies. *Optical communication technology* **2017**, *10*.
9. Garg, D.; Nain, A. Next generation optical wireless communication: a comprehensive review. *Journal of Optical Communications* **2023**, *44*, s1535–s1550.
10. Kaushal, H.; Kaddoum, G. Underwater optical wireless communication. *IEEE access* **2016**, *4*, 1518–1547.
11. Islam, S.R.; Avazov, N.; Dobre, O.A.; Kwak, K.S. Power-domain non-orthogonal multiple access (NOMA) in 5G systems: Potentials and challenges. *IEEE Communications Surveys & Tutorials* **2016**, *19*, 721–742.
12. Ding, Z.; Lei, X.; Karagiannidis, G.K.; Schober, R.; Yuan, J.; Bhargava, V.K. A survey on non-orthogonal multiple access for 5G networks: Research challenges and future trends. *IEEE Journal on Selected Areas in Communications* **2017**, *35*, 2181–2195.
13. Dai, L.; Wang, B.; Ding, Z.; Wang, Z.; Chen, S.; Hanzo, L. A survey of non-orthogonal multiple access for 5G. *IEEE communications surveys & tutorials* **2018**, *20*, 2294–2323.
14. Yin, L.; Popoola, W.O.; Wu, X.; Haas, H. Performance evaluation of non-orthogonal multiple access in visible light communication. *IEEE Transactions on Communications* **2016**, *64*, 5162–5175.
15. Tyson, R.K. Bit-error rate for free-space adaptive optics laser communications. *JOSA A* **2002**, *19*, 753–758.
16. Lee, E.J.; Chan, V.W. Part 1: Optical communication over the clear turbulent atmospheric channel using diversity. *IEEE journal on selected areas in communications* **2004**, *22*, 1896–1906.
17. Tsiftsis, T.A.; Sandalidis, H.G.; Karagiannidis, G.K.; Uysal, M. Optical wireless links with spatial diversity over strong atmospheric turbulence channels. *IEEE transactions on wireless communications* **2009**, *8*, 951–957.
18. Najafi, M.; Schmauss, B.; Schober, R. Intelligent reflecting surfaces for free space optical communication systems. *IEEE transactions on communications* **2021**, *69*, 6134–6151.
19. Minovich, A.E.; Miroshnichenko, A.E.; Bykov, A.Y.; Murzina, T.V.; Neshev, D.N.; Kivshar, Y.S. Functional and nonlinear optical metasurfaces. *Laser & Photonics Reviews* **2015**, *9*, 195–213.
20. Yu, N.; Genevet, P.; Kats, M.A.; Aieta, F.; Tetienne, J.P.; Capasso, F.; Gaburro, Z. Light propagation with phase discontinuities: generalized laws of reflection and refraction. *science* **2011**, *334*, 333–337.
21. Qian, L.; Chi, X.; Zhao, L.; Chaaban, A. Secure visible light communications via intelligent reflecting surfaces. In Proceedings of the ICC 2021-IEEE International Conference on Communications. IEEE, 2021, pp. 1–6.
22. Aboagye, S.; Ngatched, T.M.; Dobre, O.A.; Ndjiongue, A.R. Intelligent reflecting surface-aided indoor visible light communication systems. *IEEE Communications Letters* **2021**, *25*, 3913–3917.
23. Valagiannopoulos, C.; Tsiftsis, T.A.; Kovanis, V. Metasurface-enabled interference mitigation in visible light communication architectures. *Journal of Optics* **2019**, *21*, 115702.
24. Abdelhady, A.M.; Salem, A.K.S.; Amin, O.; Shihada, B.; Alouini, M.S. Visible light communications via intelligent reflecting surfaces: Metasurfaces vs mirror arrays. *IEEE Open Journal of the Communications Society* **2020**, *2*, 1–20.

25. Abumarshoud, H.; Mohjazi, L.; Dobre, O.A.; Di Renzo, M.; Imran, M.A.; Haas, H. LiFi through reconfigurable intelligent surfaces: A new frontier for 6G? *IEEE Vehicular Technology Magazine* **2021**, *17*, 37–46.
26. Glybovski, S.B.; Tretyakov, S.A.; Belov, P.A.; Kivshar, Y.S.; Simovski, C.R. Metasurfaces: From microwaves to visible. *Physics reports* **2016**, *634*, 1–72.
27. Ndjiongue, A.R.; Ngatched, T.M.; Dobre, O.A.; Haas, H. Re-configurable intelligent surface-based VLC receivers using tunable liquid-crystals: The concept. *Journal of Lightwave Technology* **2021**, *39*, 3193–3200.
28. Aboagy, S.; Ndjiongue, A.R.; Ngatched, T.M.; Dobre, O.A. Design and optimization of liquid crystal RIS-based visible light communication receivers. *IEEE Photonics Journal* **2022**, *14*, 1–7.
29. Gong, S.; Lu, X.; Hoang, D.T.; Niyato, D.; Shu, L.; Kim, D.I.; Liang, Y.C. Toward smart wireless communications via intelligent reflecting surfaces: A contemporary survey. *IEEE Communications Surveys & Tutorials* **2020**, *22*, 2283–2314.
30. Hassouna, S.; Jamshed, M.A.; Rains, J.; Kazim, J.u.R.; Rehman, M.U.; Abualhayja, M.; Mohjazi, L.; Cui, T.J.; Imran, M.A.; Abbasi, Q.H. A survey on reconfigurable intelligent surfaces: Wireless communication perspective. *IET Communications* **2023**, *17*, 497–537.
31. Hassouna, S. A Survey on Intelligent Reflecting Surfaces: Wireless Communication Perspective. *Authorea Preprints* **2023**.
32. Zheng, B.; You, C.; Mei, W.; Zhang, R. A survey on channel estimation and practical passive beamforming design for intelligent reflecting surface aided wireless communications. *IEEE Communications Surveys & Tutorials* **2022**, *24*, 1035–1071.
33. Chen, Z.; Ma, X.; Han, C.; Wen, Q. Towards intelligent reflecting surface empowered 6G terahertz communications: A survey. *China Communications* **2021**, *18*, 93–119.
34. Raza, A.; Ijaz, U.; Ishfaq, M.K.; Ahmad, S.; Liaqat, M.; Anwar, F.; Iqbal, A.; Sharif, M.S. Intelligent reflecting surface-assisted terahertz communication towards B5G and 6G: State-of-the-art. *Microwave and Optical Technology Letters* **2022**, *64*, 858–866.
35. Zhu, Y.; Mao, B.; Kato, N. Intelligent reflecting surface in 6G vehicular communications: A survey. *IEEE Open Journal of Vehicular Technology* **2022**, *3*, 266–277.
36. Mohsan, S.A.H.; Khan, M.A.; Alsharif, M.H.; Uthansakul, P.; Solyman, A.A. Intelligent reflecting surfaces assisted UAV communications for massive networks: current trends, challenges, and research directions. *Sensors* **2022**, *22*, 5278.
37. Renzo, M.D.; Debbah, M.; Phan-Huy, D.T.; Zappone, A.; Alouini, M.S.; Yuen, C.; Sciancalepore, V.; Alexandropoulos, G.C.; Hoydis, J.; Gacanin, H.; et al. Smart radio environments empowered by reconfigurable AI meta-surfaces: An idea whose time has come. *EURASIP Journal on Wireless Communications and Networking* **2019**, *2019*, 1–20.
38. Luo, S.; Hao, J.; Ye, F.; Li, J.; Ruan, Y.; Cui, H.; Liu, W.; Chen, L. Evolution of the electromagnetic manipulation: from tunable to programmable and intelligent metasurfaces. *Micromachines* **2021**, *12*, 988.
39. Ma, Q.; Bai, G.D.; Jing, H.B.; Yang, C.; Li, L.; Cui, T.J. Smart metasurface with self-adaptively reprogrammable functions. *Light: science & applications* **2019**, *8*, 98.
40. Kokdogan, F.; Gezici, S. Intelligent Reflecting Surfaces for Visible Light Positioning based on Received Power Measurements. *IEEE Transactions on Vehicular Technology* **2024**.
41. Sun, S.; Yang, F.; Song, J.; Han, Z. Joint resource management for intelligent reflecting surface-aided visible light communications. *IEEE Transactions on Wireless Communications* **2022**, *21*, 6508–6522.
42. Najafi, M.; Schober, R. Intelligent reflecting surfaces for free space optical communications. In Proceedings of the 2019 IEEE Global Communications Conference (GLOBECOM). IEEE, 2019, pp. 1–7.
43. Jamali, V.; Ajam, H.; Najafi, M.; Schmauss, B.; Schober, R.; Poor, H.V. Intelligent reflecting surface assisted free-space optical communications. *IEEE Communications Magazine* **2021**, *59*, 57–63.
44. Yang, L.; Guo, W.; da Costa, D.B.; Alouini, M.S. Free-space optical communication with reconfigurable intelligent surfaces. *arXiv preprint arXiv:2012.00547* **2020**.
45. Abumarshoud, H.; Selim, B.; Tatipamula, M.; Haas, H. Intelligent reflecting surfaces for enhanced NOMA-based visible light communications. In Proceedings of the ICC 2022-IEEE International Conference on Communications. IEEE, 2022, pp. 571–576.
46. Wang, H.; Zhang, Z.; Zhu, B.; Dang, J.; Wu, L.; Wang, L.; Zhang, K.; Zhang, Y. Performance of wireless optical communication with reconfigurable intelligent surfaces and random obstacles. *arXiv preprint arXiv:2001.05715* **2020**.

47. Wang, X.; Zhang, M.; Zhou, H.; Ren, X. Performance analysis and design considerations of the shallow underwater optical wireless communication system with solar noises utilizing a photon tracing-based simulation platform. *Electronics* **2021**, *10*, 632.
48. Cao, B.; Chen, M.; Yang, Z.; Zhang, M.; Zhao, J.; Chen, M. Reflecting the light: Energy efficient visible light communication with reconfigurable intelligent surface. In Proceedings of the 2020 IEEE 92nd Vehicular Technology Conference (VTC2020-Fall). IEEE, 2020, pp. 1–5.
49. Sun, S.; Yang, F.; Song, J. Sum rate maximization for intelligent reflecting surface-aided visible light communications. *IEEE Communications Letters* **2021**, *25*, 3619–3623.
50. Naik, R.P.; Chung, W.Y. Evaluation of reconfigurable intelligent surface-assisted underwater wireless optical communication system. *Journal of Lightwave Technology* **2022**, *40*, 4257–4267.
51. Wu, Q.; Zhang, J.; Guo, J. Capacity maximization for reconfigurable intelligent surface-aided MISO visible light communications. In Proceedings of the Photonics. MDPI, 2022, Vol. 9, p. 487.
52. Zhan, L.; Zhao, H.; Zhang, W.; Lin, J. An optimal scheme for the number of mirrors in vehicular visible light communication via mirror array-based intelligent reflecting surfaces. In Proceedings of the Photonics. MDPI, 2022, Vol. 9, p. 129.
53. Ata, Y.; Abumarshoud, H.; Bariah, L.; Muhaidat, S.; Imran, M.A. Intelligent reflecting surfaces for underwater visible light communications. *IEEE Photonics Journal* **2023**, *15*, 1–10.
54. Chen, C.; Huang, S.; Abumarshoud, H.; Tavakkolnia, I.; Safari, M.; Haas, H. Frequency-domain channel characteristics of intelligent reflecting surface assisted visible light communication. *Journal of Lightwave Technology* **2023**.
55. Qian, L.; Zhao, L.; Huang, N.; Chaaban, A.; Xu, Z. Security enhancement by intelligent reflecting surfaces for visible light communications. *Optics Communications* **2024**, p. 130851.
56. Li, Q.T.; Dong, F.; Wang, B.; Gan, F.; Chen, J.; Song, Z.; Xu, L.; Chu, W.; Xiao, Y.F.; Gong, Q.; et al. Polarization-independent and high-efficiency dielectric metasurfaces for visible light. *Optics express* **2016**, *24*, 16309–16319.
57. Tao, J.; You, Q.; Yang, C.; Li, Z.; Deng, L.; Wu, M.; Luo, M.; Wu, L.; Li, C.; Liu, Z.; et al. Beam-steering metasurfaces assisted coherent optical wireless multichannel communication system. *Nanophotonics* **2023**, *12*, 3511–3518.
58. Khalid, R.; Wu, Q.Y.S.; Mahmood, N.; Deng, J.; Nematic, A.; Valiyaveedu, S.K.; Cabrera, H.; Mehmood, M.Q.; Teng, J.; Zubair, M. Fluid-Responsive Tunable Metasurfaces for High-Fidelity Optical Wireless Communication. *Materials Horizons* **2024**.
59. Ndjiongue, A.R.; Ngatched, T.M.; Dobre, O.A.; Haas, H. Toward the use of re-configurable intelligent surfaces in VLC systems: Beam steering. *IEEE Wireless Communications* **2021**, *28*, 156–162.
60. Shirmanesh, G.K.; Sokhoyan, R.; Wu, P.C.; Atwater, H.A. Electro-optically tunable multifunctional metasurfaces. *ACS nano* **2020**, *14*, 6912–6920.
61. Tao, J.; You, Q.; Li, Z.; Luo, M.; Liu, Z.; Qiu, Y.; Yang, Y.; Zeng, Y.; He, Z.; Xiao, X.; et al. Mass-Manufactured Beam-Steering Metasurfaces for High-Speed Full-Duplex Optical Wireless-Broadcasting Communications. *Advanced Materials* **2022**, *34*, 2106080.
62. Mermet-Lyaudoz, R.; Combeau, P.; Drouard, E.; Julien-Vergonjanne, A.; Seassal, C.; Nguyen, H.S.; Sahuguede, S. Multiscale simulation for visible light communication using perovskite metasurface. In Proceedings of the 2021 17th International Symposium on Wireless Communication Systems (ISWCS). IEEE, 2021, pp. 1–6.
63. Hu, Y.; Ou, X.; Zeng, T.; Lai, J.; Zhang, J.; Li, X.; Luo, X.; Li, L.; Fan, F.; Duan, H. Electrically tunable multifunctional polarization-dependent metasurfaces integrated with liquid crystals in the visible region. *Nano letters* **2021**, *21*, 4554–4562.
64. Cao, Z.; Zhang, X.; Osnabrugge, G.; Li, J.; Vellekoop, I.M.; Koonen, A.M. Reconfigurable beam system for non-line-of-sight free-space optical communication. *Light: Science & Applications* **2019**, *8*, 69.
65. Hu, J.; Guo, Z.; Shi, J.; Jiang, X.; Chen, Q.; Chen, H.; He, Z.; Song, Q.; Xiao, S.; Yu, S.; et al. A metasurface-based full-color circular auto-focusing Airy beam transmitter for stable high-speed underwater wireless optical communications. *Nature Communications* **2024**, *15*, 2944.

**Disclaimer/Publisher's Note:** The statements, opinions and data contained in all publications are solely those of the individual author(s) and contributor(s) and not of MDPI and/or the editor(s). MDPI and/or the editor(s) disclaim responsibility for any injury to people or property resulting from any ideas, methods, instructions or products referred to in the content.